



Outlet of the Fan for Overcoming the Suction Limit of Fan Law

Chul Hwan Seul

Abstract

Ventilation systems are crucial for controlling the indoor air quality in closed spaces and mitigating health hazards. However, for a high suction performance, fan-based ventilation requires considerable energy consumption along with subsequent environmental and financial drawbacks. According to the Dalla Valle physical theory, which is a universal physical law applied to fans, it is impossible to achieve air suction beyond the fan's inherent output capacity or to change the suction pattern. However, this research introduces a method to overcome the Dalla Valle physical equation through suction beyond the fan's inherent output capacity and changes in the fan's suction pattern. Our method combines the use of a bladeless fan in series with an axial fan to exploit airflow dynamic properties and increase the output efficiency. Our findings show that the proposed fan configuration provides a new foundation for developing improved ventilation systems to overcome the limitations of fan laws.

Introduction

Air pollution is an important concern for global environment protection efforts and policies [1–6]. For decades, international research and development activities have been focused on reducing outdoor air pollution factors in large cities caused by various industries and transportation modes [7–13]. The coronavirus 2019 (COVID-19) pandemic created a fundamental shift in the air quality landscape, garnering unprecedented attention to the importance of indoor air quality [14–17], and the correct ventilation of indoor spaces is critical for preventing the uncontrollable spread of COVID-19 [18–20]. Nevertheless, indoor ventilation systems, with a multitude of configurations, have been investigated over the years owing to their fundamental role in controlling health hazards. Numerous studies have addressed improving ventilation in hospitals and clinics [21,22], schools [23–25], closed public spaces (e.g., libraries and malls) [26,27], laboratories [28–30], workplaces [31,32], and kitchens [33–35]. Ventilation systems for indoor spaces are used to improve the air quality of enclosed areas by removing particulate contaminations [36–40] and smoke [22,28,39,40], controlling humidity [41,42], dissipating heat [36,43], or a combination of all these applications.

Designing of an efficient ventilation solution involves a complex combination of parameters and boundary conditions to achieve the adequate airflows at reasonable energy and power costs. The choice of fan is crucial for defining the performance of any given ventilation system, which involves the propeller (or impeller) type, dimensions, rotational speed, and blade configurations [44,45]. These parameters affect and define the volume and flow of air managed by the ventilation system. In addition, static and dynamic air pressures impose considerable constraints on the selection of fan parameters

Affiliation:

Independent Researcher, 201 25-12, Chojung 11-gil, Jeungpyeong-eup, Jeungpyeong-gun, Chungcheongbuk-do, Republic of Korea

*Corresponding author:

Chul Hwan Seul, 201 25-12, Chojung 11-gil, Jeungpyeong-eup, Jeungpyeong-gun, Chungcheongbuk-do, Republic of Korea

Citation: Chul Hwan Seul. Independent Researcher, 201 25-12, Chojung 11-gil, Jeungpyeong-eup, Jeungpyeong-gun, Chungcheongbuk-do, Republic of Korea. Archives of Microbiology and Immunology. 9 (2025): 171-178.

Received: May 15, 2025

Accepted: May 19, 2025

Published: May 23, 2025

for a given ventilation system [46]. For instance, in ducted solutions, where the exhaust of a ventilation fan is connected to a duct, the exhausted air experiences high-pressure conditions to overcome frictions in the duct. These conditions impose totally different requirements on the fan design and power resources compared with those of ductless ventilations [47–50]. Currently, ventilation systems with higher airflow, air volume, and pressure demands are usually addressed by increasing rotational speeds or fan dimensions or parallelly using multiple fans [47,51–54]. Although these approaches can meet the ventilation solution demands, they impose considerable energetic and financial limitations [42,51–55]; additionally, noise problems and stability issues become prominent when larger fans are use [56]. Finding a compromise solution for high ventilation performances at low resource cost is usually a bottleneck in designing fan configuration. Herein, we propose a new fan configuration to improve the airflow suction performance of a ventilation system with no additional energy requirements. The proposed solution uses dual fans in series, substantially increasing the overall airflow suction efficiency while the power consumption is restricted to the first fan only. We demonstrate that a combination of the first fan suction with airflow dynamics and Bernoulli's law markedly improves the suction efficiency at the output of the second fan. The proposed system is expected to provide the foundation for novel ventilation solutions to overcome the existing challenges imposed by empirical physical laws applied to fans.

Theoretical Background

Axial fans (with an axial impeller) have pitched blades attached to a central rotating hub. Upon rotation of the entire

assembly, the pitched blades push against air to create a pressure differential that induces air to flow from the high-pressure region to the low-pressure region, known as the induced flow. The airflow direction depends on the direction of the blades' rotation. For clockwise-rotating blades, air is pushed forward from the face of the fan, whereas in counterclockwise rotation, air is pushed backward. Axial fans are commonly used for ventilation applications requiring high airflow rates and low-pressure conditions, such as nonducted indoor ventilation. In axial fans, the airflow rate is usually increased by increasing the rotational speed of blades. Nevertheless, the volume of air flowing through the fan is limited by the size of its blades, as shown in Figure 1.

Figure 4. Experimentally measured air velocity in two fans in a serial configuration, showing the effect of the air velocity of the induced flow on the air intake volume as a function of the distance between the first and second fans.

A set of equations dictate the relationships between the rotational speed (ω) of the fan blades (expressed in rounds per minute), volumetric flow rate (Q), static pressure (P_s), and horsepower (H_p) required to drive the fan. These equations define the so-called fan laws as follows:

$$\frac{Q_1}{Q_0} = \frac{\omega_1}{\omega_0}, \# \quad [1]$$

$$\frac{P_{s1}}{P_{s0}} = \left(\frac{\omega_1}{\omega_0} \right)^2, \# \quad [2]$$

$$\frac{H_{p1}}{H_{p0}} = \left(\frac{\omega_1}{\omega_0} \right)^3, \# \quad [3]$$

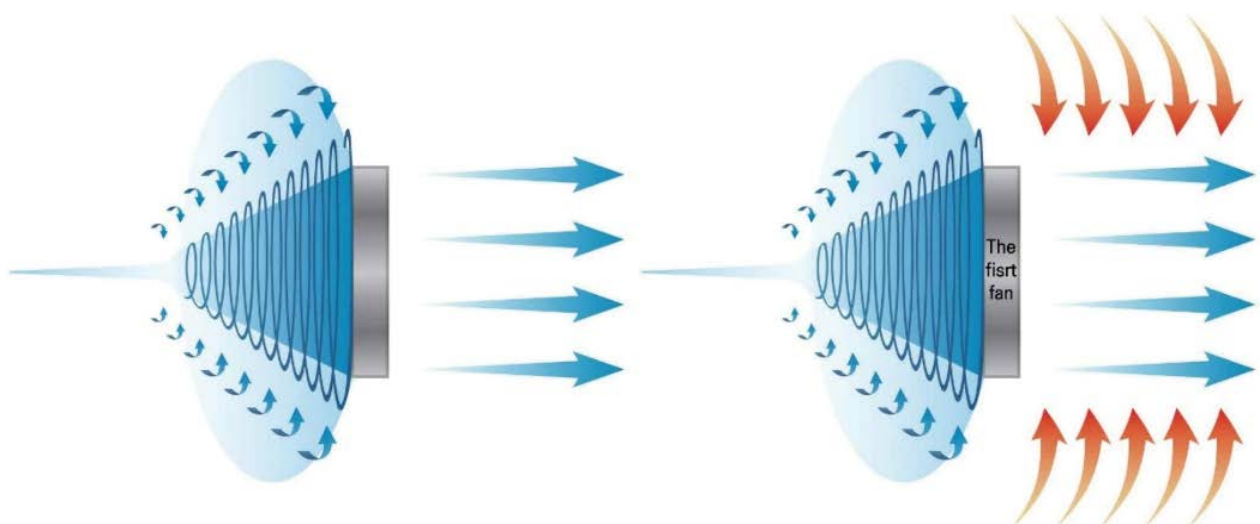


Figure 1: (a) Representation of the effect of the rotational motion of the fan blades on the air volume at the front, also showing that the air intake and output are equal. (b) Visualization of the airflow induced from the front (left) input to the rear (right) output (or exhaust) of the fan. The green arrow indicates the airflow caused by the fan's discharge. The red arrow indicates the additional airflow caused by air turbulence at the boundary of the fan exhaust, which is a focal point of this study and the key to overcoming the limitations of the Dalla Valle physics.

where, Q_0 , P_{s0} , and H_{p0} correspond to an initial state and, Q_f , P_{sf} , and H_{pf} correspond to a final state. Therefore, the increase in the volumetric airflow rate is directly proportional to the increase in the rotational speed of the blades. Thus, to double the flow rate, the speed of the fan must be equally doubled. However, increasing the volumetric flow rate requires exponential variations of the required horsepower to drive the fan. According to equations 1 and 3, to increase the flow rate by 50%, the horsepower has to be increased by 237%. Hence, increasing the suction performance of a ventilation fan imposes dramatic energy costs.

The efficiency (ζ) of a fan is determined by the airflow rate (Q), total pressure (P_t), and input

horsepower (H_{pi}) used to drive the fan as follows:

$$\zeta = \frac{Q \times P_t}{H_{pi}}, \# \quad [4]$$

The total pressure of the fan (P_t) is defined by the loss pressure (P_{loss}) and velocity pressure at the fan outlet ($P_{v,out}$), which is given by:

$$P_t = P_{loss} + P_{v,out}, \# \quad [5]$$

where P_{loss} results from dynamic, component, and frictional pressure losses through the air system. For an ideal fan in a ductless system, $P_{loss} = 0$. The static pressure P_s is related to the total pressure by:

$$P_s = P_t - P_{discharge}, \# \quad [6]$$

where $P_{discharge}$ corresponds to the velocity pressure of the fan discharge, relative to the cases of ducted systems for example. For a ductless system (e.g., the fan in Figure 1), the static pressure is equal to the total pressure as $P_{discharge} = 0$. Using the expressions in equations 4 and 6, the efficiency of a

ventilation fan can be improved by increasing the volumetric airflow rate (Q) and/or static pressure (P_s) and by decreasing the horsepower at the input (H_{pi}) of the system. In our approach presented herein, the volumetric airflow rate (Q) is increased by placing two fans in series. The energy from the fan1 output airflow is used as the input flow for fan2, while the main input horsepower is dictated by that of fan1. This system consequently provides important improvements in the ventilation fan efficiency.

Method

Fan configuration

In the proposed method, two fans are placed in series (Figure 2). The first fan (fan1) on the left is a blade fan with an axial propeller, while the second fan (fan2) on the right is bladeless. The two fans have equal radii and are positioned in series on the same central axis. Figure 2 shows a schematic representation of this configuration and indicates the vortex formed at the inlet of fan1, resulting from the rotational motion of the blades.

The airflow output of fan1 is directed toward the input of fan2, where its flow energy is used to increase the input volumetric airflow rate of fan2. Using the accelerated airflow from the output of fan1 as an input flow for fan2 constitutes the core of the proposed approach. Nevertheless, the air dynamics between the two fans and the geometric configuration of the whole assembly (i.e., size of fans and separation distance) are crucial in improving the overall volumetric airflow rate at the final output of the system (i.e., output of fan2). Although, the main input horsepower remains tightly dependent on that of fan1, the efficiency of this dual-fan series ventilation system is expected to exhibit a significant improvement.

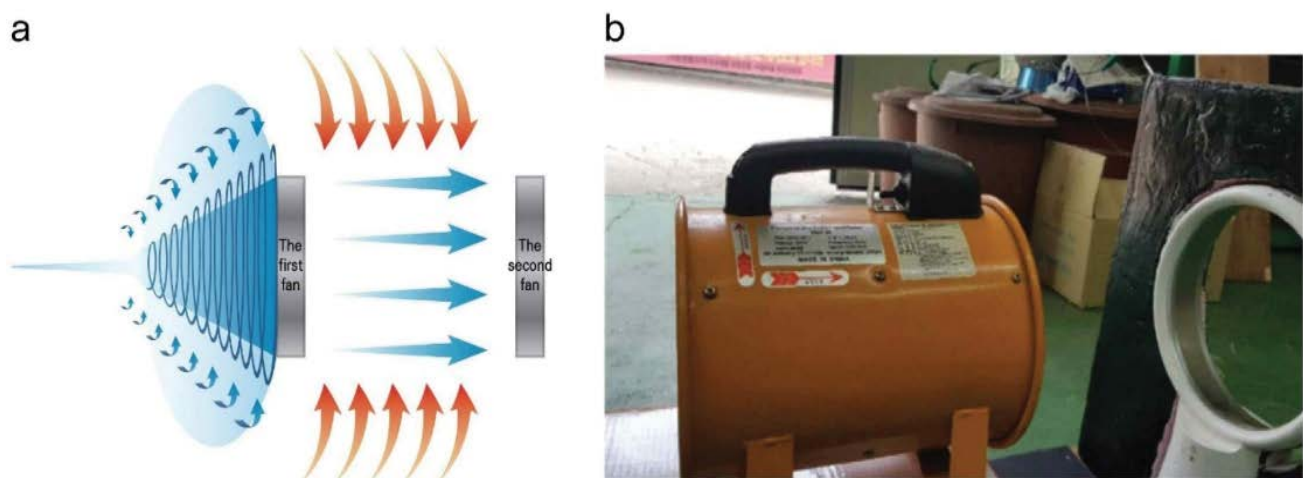
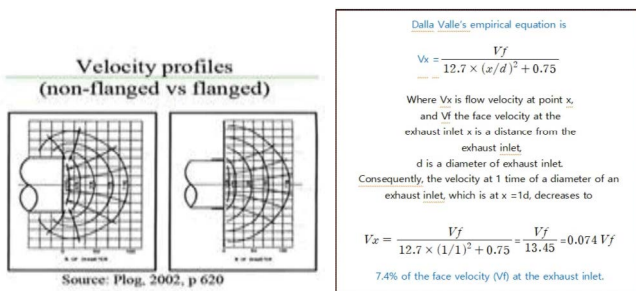


Figure 2: (a) Schematic of the two-fan configuration proposed in this study. The first fan (left) is a blade fan with an axial propeller while the second fan (right) is a bladeless fan. Both fans have the same radius and are placed along the same central axis (b) Photograph of the two fans used for testing.

Volumetric airflow

To understand the contributions of aerodynamic phenomena and fan configurations to the expected improvement in the ventilation fan efficiency, the volumetric airflow across the whole system is depicted in Figure 3. Three distinct regions are considered in this case. Region 1 corresponds to the air volume affected by the rotational energy of the blades in fan1, representing the input volumetric airflow rate Q_1 . Being an axial blade, the suction performance of the fan1 obeys the empirical law derived by Dalla Valle in 1952.



Depending on the radius of the fan blades, the air velocity decays exponentially with the distance from the front of the fan, reaching ~7.4% of its face velocity (i.e., at the vicinity of the fan) at a distance equal to that of the diameter of the blades [46]. Therefore, the effective volume of air flowing to the input of the fan1 can be approximated using a cone shape, whose base radius equals that of the blades (r) and height $h = 2r$. Thus, the volume of air at the input of fan1 is given by:

$$V_1^{input} = \pi r^2 \frac{h}{3} = \frac{2}{3} \pi r^3, \# \quad [7]$$

By placing the second fan at a distance d behind the first fan, a somewhat confined intermediate region is obtained, which can be defined using a cylindrical shape (i.e., region 2). The volume of this region is determined by the radius of fan1 and distance separating the two fans, as follows:

$$V_2 = \pi r^2 d, \# \quad [8]$$

As fan 2 and fan1 have the same radius and are positioned along the same central axis, the volume of air at the exit of the second fan (i.e., region 3) is approximately equal to that of the air in region 2. Thus,

$$V_3^{output} \approx V_2, \# \quad [9]$$

Using the expressions in equations 7–9, the increase in the volume of air flowing at the output of the system (i.e., output of fan 2) relative to that flowing at the input (i.e., input of fan 1) is estimated. Selected values of the blades radius and distance between the two fans are shown in Table 1.

Table 1 provides an estimated insight into the significant increase in the overall efficiency of the ventilation system proposed in Figure 2. Although the calculations suggest that

Table 1: Estimation of the increase in air volume at the output of the dual-fan system based on selected values of the blade radius and distance separating the two fans.

Blade radius, r (cm)	Distance, d (cm)	출판팬출판팬출판팬/ 출판팬출판
15	15	150%
	30	300%
30	30	150%
	60	300%

the increase in the volume ratio is simply proportional to the distance between the fans, the efficiency depends directly on the volumetric airflow rate (equation 4), rather than the air volume. For this, it is critical to consider the air dynamics phenomena contributing to the variations in the airflow rate in regions 2 and 3 (Figure 3). Air exiting fan 1 enters the region 2 with a given acceleration, generating a low-pressure zone in this region relative to the surrounding atmosphere. Following Bernoulli's law, an additional airflow will occur due to induction from high-pressure zones to the low-pressure zone in the region 2 (red arrows in Figure 3). Therefore, the volumetric airflow rate in region 2 increases relative to that in region 1. Similarly, the airflow rate in region 3 increases relative to that in region 2 due to a combination of the following three factors. First, the airflow is drawn through the bladeless fan by induction, caused by the pressure differential created by the accelerated air. Second, owing to its design, the cross-section shape of the ring in fan2 resembles that of an airplane wing. Air entering the slits of the bladeless ring accelerates because of the Coanda effect and consequently draws in more airflow in accordance with Bernoulli's law. Finally, as air exits the discharge frame of the bladeless fan, it creates local turbulences around the boundaries of region 3, causing additional airflow to enter this zone. When used separately, a bladeless fan is known to increase its output airflow rate by approximately 16-fold relative to the input airflow at the base fan.

Therefore, the combination of all the factors mentioned above indicates that the volumetric airflow rate at the final output of the system is considerably increased with respect to its value at the input of the system. Consequently, the efficiency of the setup proposed in this study is dramatically enhanced, based on equation 4.

In this study, we examined the air flow velocity of two fans connected in series to enhance the overall suction efficiency beyond the classical constraints of the Dalla Valle equation, which is typically associated with single-fan suction systems. The proposed methodology involved positioning a primary axial ventilation fan in alignment with a secondary bladeless fan, maintaining an adjustable distance between them. Although the air suction at the intake of the first fan adheres to the Dalla Valle equation, the present findings revealed

that air flow velocity at its output maintains elevated levels over considerable distances. As a result, the expansion of the induced flow caused by the distance between the first and the second fan increases the air intake of the second fan by a maximum of 25%. This is expected to enable the development of a more efficient suction ventilation system that uses similar power resources but with higher performance.

Results and Discussion

In this study, we experimentally tested the two-fan series configuration by measuring the air velocity and air flow using an anemometer (GM816, BENETECH, China). To this end, we used a heavy-duty portable axial-fan ventilator (SMP-20, SMATO) with blades (span size: 20 cm; rotational speed: 2800–3300 rpm) as the first fan (fan1). The second fan (fan2) used in these tests include a typical commercial bladeless fan. The test results associated with the different regions described in Figure 3 are further presented in Figure 4.

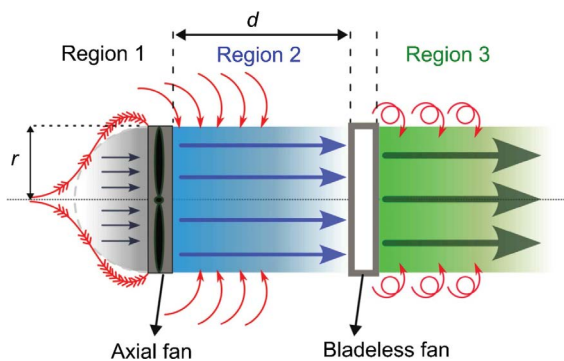


Figure 3: Schematic of the air volume flowing in different regions defined by the boundary conditions in the proposed configuration of the two fans in series. Blue is the air intake and discharge area of dalla valle, a universal physical law applied to fans, and red is the induced flow generated during discharge.

The air velocity at the inlet of fan1 is recorded at approximately 28–30.9 km/h, which decreases to 5.7 km/h at a distance equivalent to the diameter of the fan blades (i.e., 20 cm). Near the outlet of fan1, the air retains its initial velocity (~28–30.9 km/h). The velocity in the area behind fan1, influenced by the lateral pressure differential (indicated by red arrows), is measured at 4.3, 3.5, and 3.2 km/h, increasing with the distance from the rear of fan1. Notably, the air at the output of the fan1 sustains higher velocities over greater distances than at the inlet of the fan1. The measurements indicated air velocities of ~26–28 km/h at a 20 cm distance from the fan, reducing to ~18–21 km/h at 40 cm, which is double the blade diameter.

These findings suggest that the air exiting fan1 exhibits remarkably high velocities over extended distances in the confined space between the two fans compared to the intake region velocities.

Subsequently, the air intake for fan2, positioned in series with fan1, demonstrates a 25% enhancement over the intake of fan1. This series arrangement leads to a marked increase in air velocity and volume at the intake of fan2, surpassing the empirical constraints of the Dalla Valle equation. The discharge capacity of the combined setup at the output of fan2 displays substantial improvement over a single fan system. This enhancement is evident in experimental recordings comparing a single fan setup (<https://www.youtube.com/watch?v=QLc6Xb9nTpc>) and a dual-fan

series setup (<https://www.youtube.com/watch?v=Izoh9gOB8Ek>). Notably, the extensive increase

in the induced discharge flow in the latter setup induces an unusual rotational air suction near the front of the fan1. The cause of this phenomenon remains unclear. However, Figure 4 suggests that adjusting the distance between the

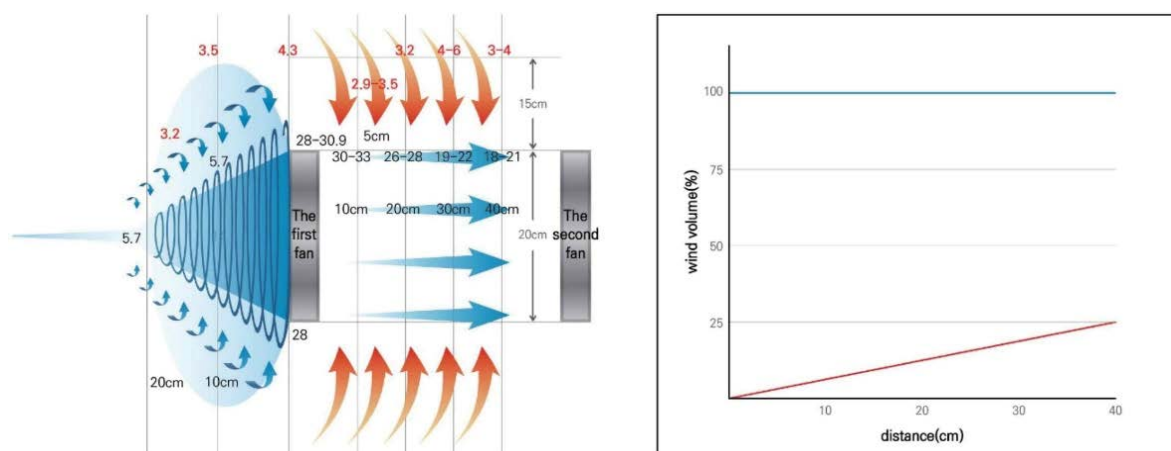


Figure 4. A Experimentally measured air velocity in two fans in a serial configuration, showing the effect of the air velocity of the induced flow on the air intake volume as a function of the distance between the first and second fans. B It shows that the amount of air inflow is determined by the inflow speed of the air.

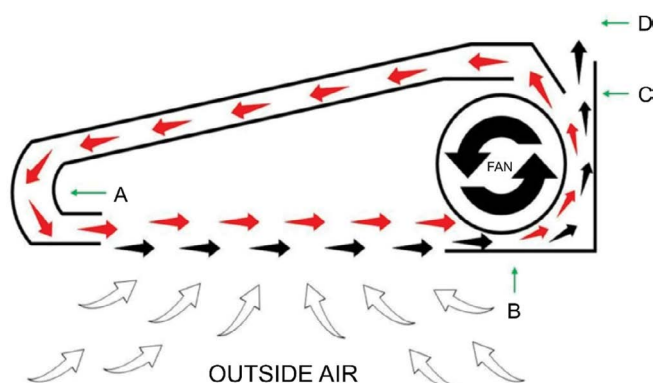


Figure 5: Fan configuration of an improved large oven suction system based on the main concept presented in this study.

two fans can increase air intake at fan2 without modifying the blades, thereby enhancing the performance with the same power resources. The fan configuration proposed in this study leverages the airflow dynamics between two points using two fans. This approach is applicable for enhancing particulate matter suction and air quality in closed kitchen spaces, particularly in large cooking ovens. Figure 5 presents a schematic of the suggested oven fan configuration, drawing from the principles discussed in this study.

In conventional configurations of kitchen ventilation systems, a fan with a large and fast rotational force can actively suck in polluted air. However, when the size of the emission pipe is fixed, the motor capacity or fan size should not be increased. In the proposed configuration (Figure 5), air sucked in by the rotational force of the cross-flow fan at point B is separated into exhaust and circulating air, which moves to point D along a 100 mm pipe and point A. The circulating air traveling to point A further moves to point B. This infinite airflow from points A, B, and C forms an air belt and creates a wide range of induced airflow around the range hood. In addition, the separation of circulating and exhaust air resolves the limitation due to the suction amount and exhaustion in a conventional range hood.

Conclusion

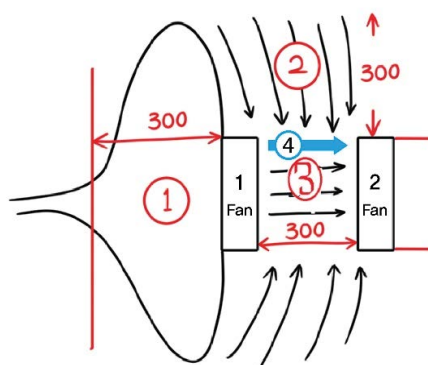


Figure 6

The air suction area of dalla valle, a universal physical law—commonly applied to fan suction—is shown as area 1 in the figure. The corresponding discharge is denoted as 3, and the suction power of 1 and the discharge amount of 3 are equal. However, 2 is separate from the air suction of 1; it utilizes the rapid airflow generated during the discharge at 1 by placing a secondary fan. It was possible to convert the fan's inherent functions of suction, discharge, and the resulting flow into a new form of air intake. Here, if the air suction speed in <Figure 1> is doubled, the energy consumption generally increases by 8 times. This is because the energy consumption of compressed air is proportional to the cube of the suction speed. However, in 4 of <Figure 1>, no additional energy is required. The discharge itself involves a rapid airflow equal to the intake velocity, which in turn contributes to an increase in suction speed. Additionally, through the expansion of the fluid volume in 2, and due to the presence of a similarly fast airflow as the intake speed—like in 4 of <Figure 1>—an unusual rotating air intake was observed near the front of the fan. This phenomenon is presumed to be caused by the accelerated air movement and the volumetric expansion occurring in 2.



This research shows that when air continuously moves quickly from point A to point B, a flow occurs between A and B, which is observed at the fan's outlet. Additionally, the flow concentrates surrounding air to point C, which enables overcoming the limitations of the Dalla Valle physical equation, which is the universal physical law applied to fan suction.

Acknowledgments

The authors thank Crimson Interactive Pvt. Ltd. (Enago) for their assistance in manuscript editing. And I would like to thank Joohee kang for helping with the English translation.

Funding

This research did not receive any specific grant from public, commercial, or not-for-profit sectors

Author Contribution

The author confirms sole responsibility for the following: study conception and design, data collection, analysis and interpretation of results, and manuscript preparation.

Data Availability Statement

The datasets generated during and/or analysed during the current study are available from the corresponding author on reasonable request.

Competing Interests

The authors have no conflict of interests to declare.

References

1. Wilker EH, Osman M & Weisskopf MG. Ambient air pollution and clinical dementia systematic review and meta-analysis. *BMJ* 381 (2023): e071620.
2. Sicard P, et al. Trends in urban air pollution over the last two decades: A global perspective. *Sci. Total Environ* 858 (2023): 160064.
3. Thompson R, et al. Air pollution and human cognition: A systematic review and meta- analysis. *Sci. Total Environ* 859 (2023): 160234.
4. Cory-Slechta DA, Merrill A & Sobolewski M. Air pollution–related neurotoxicity across the life span. *Annu. Rev. Pharmacol. Toxicol* 63 (2023): 143-163.
5. Hicken MT, Payne-Sturges D & McCoy E. Evaluating race in air pollution and Health Research: race, PM2.5 air pollution exposure, and mortality as a case study. *Curr. Environ. Heal. Rep* 10 (2023): 1-11.
6. Pozzer A, et al. Mortality attributable to ambient air pollution: a review of global estimates *Geo health* 7 (2023): e2022GH000711.
7. Lin Y, Huang R & Yao X. Air pollution and environmental information disclosure: an empirical study based on heavy polluting industries. *J. Clean. Prod* 278 (2021): 124313.
8. Rentschler J & Leonova N. Global air pollution exposure and poverty. *Nat. Commun* 14 (2023): 4432.
9. Cole MA. Air pollution and ‘dirty’ industries: how and why does the composition of manufacturing output change with economic development? *Environ. Resour. Econ* 17 (2000): 109-123.
10. Colville RN, Hutchinson EJ, Mindell JS & Warren RF. The transport sector as a source of air pollution. *Atmos. Environ* 35 (2001): 1537-1565.
11. Cepeda, M. et al. Levels of ambient air pollution according to mode of transport: a systematic review. *Lancet Public Health* 2 (2017): e23-e34.
12. Krämer U, Koch T, Ranft U, et al. Traffic-related air pollution is associated with atopy in children living in urban areas. *Epidemiology* 11 (2000): 64-70.
13. Borrego C, et al. Traffic-related particulate air pollution exposure in urban areas. *Atmos. Environ* 40 (2006): 7205-7214.
14. Elsaid AM & Ahmed MS. Indoor air quality strategies for air-conditioning and ventilation systems with the spread of the global coronavirus (COVID-19) epidemic: improvements and recommendations. *Environ. Res.* 199 (2021): 111314.
15. Abouleish MYZ. Indoor air quality and COVID-19. *Public Health* 191 (2021): 1-2.
16. Bidilă T, Pietraru RN, Ioniță AD & Olteanu A. Monitor indoor air quality to assess the risk of COVID-19 transmission. 23rd Int. Conf. Control. Syst. Comput. Sci (2021): 356-361.
17. Fernández-Agüera J, Domínguez-Amarillo S, Campano MÁ & Al-Khatiri H. Effects of covid-induced lockdown on inhabitants’ perception of indoor air quality in naturally ventilated homes. *Air Qual. Atmos. Health* 16 (2023): 193-212.
18. Buonomano A, Forzano C, Giuzio GF & Palombo A. New ventilation design criteria for energy sustainability and indoor air quality in a post Covid-19 scenario. *Renew. Sustain. Energy Rev* 182 (2023): 113378.
19. Moghadam TT, Ochoa Morales CEO, Lopez Zambrano MJ, Bruton K, et al. Energy efficient ventilation and indoor air quality in the context of COVID-19 - A systematic review. *Renew. Sustain. Energy Rev* 182 (2023): 113356.
20. Wiryasaputra R, et al. Review of an intelligent indoor environment monitoring and management system for COVID-19 risk mitigation. *Front. Public Heal* 10 (2022): 1022055
21. Kermenidou M, et al. Determination of particulate matter in dental clinics: the effectiveness of different air purifiers and the central ventilation system. *Indoor Air* (2023): 1-18.
22. Liu Z, et al. Quantitative evaluation of the transmission and removal of harmful smoke particles in the operating room: full-scale experimental and numerical study. *Indoor Air* (2023): 1-17.
23. Dorizas PV, Assimakopoulos MN, Helmis C, & Santamouris M. An integrated evaluation study of the ventilation rate, the exposure and the indoor air quality in naturally ventilated classrooms in the Mediterranean region during spring. *Sci. Total Environ.* 502 (2015): 557-570.
24. Trompetter WJ, et al. The effect of ventilation on air particulate matter in school classrooms. *J. Build. Eng.* 18 (2018): 164-171.
25. Guo M, et al. Effects of increasing indoor negative air ions on cognitive performance and health of high pure CO2 level-exposed college students. *Indoor Air* (2023): 1-11.
26. Du W, et al. Attached smoking room is a source of PM2.5 in adjacent nonsmoking areas. *Indoor Air* (2023): 1-8.
27. Śmiełowska M, Marć M & Zabiegała B. Indoor air quality in public utility environments—a review. *Environ. Sci. Pollut. Res. Int.* 24 (2017): 11166-11176.
28. Rumchev K, van den Broeck V & Spickett J. Indoor air

- quality in university laboratories. *Environ. Heal* 3 (2003): 11-19.
29. Di Giulio M, Grande R, Di Campli E, Di Bartolomeo S & et al. Indoor air quality in university environments. *Environ. Monit. Assess* 170 (2010): 509-517.
 30. Memarzadeh F. Effect of reducing ventilation rate on indoor air quality and energy cost in laboratories. *J. Chem. Health Saf* 16 (2009): 20-26.
 31. Carrer, P. & Wolkoff, P. Assessment of indoor air quality problems in office-like environments: role of occupational health services. *Int. J. Environ. Res. Public Health* 15 (2018).
 32. Chau CK, Hui WK & Tse MS. Evaluation of health benefits for improving indoor air quality in workplace. *Environ. Int* 33 (2007): 186-198.
 33. Kang K, Kim T & Kim DD. An investigation of concentration and health impacts of aldehydes associated with cooking in 29 residential buildings. *Indoor Air* (2023): 1-18.
 34. Ditto JC, et al. Indoor and outdoor air quality impacts of cooking and cleaning emissions from a commercial kitchen. *Environ. Sci. Process Impacts* 25 (2023): 964-979.
 35. Zakaria IB, Mahyuddin N & Mohd-Sahabuddin MF. Kindergarten physical setting guidelines. Kindergarten physical setting guidelines: a review from indoor air quality perspectives. *E3S Web of Conf* 396 (2023).
 36. Sheng Y, Fang L & Nie J. Experimental analysis of indoor air quality improvement achieved by using a clean-air heat pump (CAHP) air-cleaner in a ventilation system. *Build Environ* 122 (2017): 343-353.
 37. Gallego E, Roca X, Perales JF & Guardino X. Determining indoor air quality and identifying the origin of odour episodes in indoor environments. *J. Environ. Sci. (China)* 21 (2009): 333-339.
 38. Canha N, Lage J, Candeias S, Alves C & Almeida SM. Indoor air quality during sleep under different ventilation patterns. *Atmos. Pollut. Res* 8 (2017): 1132-1142.
 39. Li L, et al. Molecular characteristics, sources, and health risk assessment of gaseous carbonyl compounds in residential indoor and outdoor environments in a megacity of Northwest China. *Indoor Air* (2023): 1-13.
 40. Muthukrishnan P & Farahi F. Effects of ionization on the filtration of fine and ultrafine particles in indoor air. *Indoor Air* (2023): 1-7.
 41. Sekhar SC. Space temperature difference, cooling coil and fan—energy and indoor air quality issues revisited. *Energy Build* 37 (2005): 49-54.
 42. Yang JK, et al. Performance and economic efficiency analysis of an integrated, outdoor fan-ventilated cooling device. *Heliyon* 9 (2023): e13927.
 43. Wiriyasart S & Naphon P. Numerical study on air ventilation in the workshop room with multiple heat sources. *Case Stud. Therm. Eng* 13 (2019): 100405.
 44. Bamberger, K., Carolus, T. & Haas, M. Optimization of low-pressure axial fans and effect of subsequent geometrical modifications, *FAN 2015. Int. Conf. Fan Noise, Technol. Numer. Methods*, 1-10 (2015).
 45. Wang J & Kruyt NP. Design for high efficiency of low-pressure axial fans with small hub-to-tip diameter ratio by the vortex distribution method. *J. Fluids Eng. Trans. ASME* 144 (2022).
 46. Plog BA. ed. *Fundamentals of industrial hygiene*. 5th ed (National Safety Council Press (2003).
 47. G. Guidelines. Design of fan-assisted natural ventilation general guidelines and suggested design for design of fan-assisted natural ventilation (1997).
 48. Auld G. An estimation of fan performance for leaky ventilation ducts. *Undergr. SP Technol* 19 (2004): 539-549.
 49. Przydróżny E, Przydróżna A & Szczęśniak S. Energy efficient setting of supply air temperature in dual-duct dual-fan ventilation systems with extract air recirculation. *Sci. Eng. Progr* 5 (2018): 69-85
 50. Entry Losses, Ducts and Hoods (nd).
 51. USDOE. Improving fan system performance: A sourcebook for Industry, U.S. Dep. Energy 83 (2003).
 52. Ruano AF. Design of a ventilation system for fan testing (University of Valladolid. School of Industrial Engineering, Vives University College Kortrijk (2017).
 53. Bamberger K & Carolus T. Design guidelines for low pressure axial fans based on CFD- trained meta-models. 11th Eur. Conf. Turbomach. Fluid Dyn. Thermodyn. ETC (2015).
 54. Corona JJ, Mesalhy O, Chow L, et al. The best efficiency point of an axial fan at low-pressure conditions. *Adv. Mech. Eng* 13 (2021): 1-17.
 55. Awbi HB. Ventilation for good indoor air quality and energy efficiency. *Energy Procedia* 112 (2017): 277-286.
 56. Zhao Y, Xu C, Zheng Z, et al. Experimental study of the parameter effects on the flow and noise characteristics for a contra-rotating axial fan. *Front. Phys* 11 (2023): 1-13.



This article is an open access article distributed under the terms and conditions of the [Creative Commons Attribution \(CC-BY\) license 4.0](https://creativecommons.org/licenses/by/4.0/)